

- 4 (d) 1  $x, y, z; \bar{x}, y, \bar{z}; 1/2 - x, y, z;$   
 $1/2 + x, y, \bar{z} \pmod{n, n', n''};$   
 2 (c) m  $1/4, y, z; 3/4, y, \bar{z} \pmod{n, n', n''};$   
 2 (b) 2  $0, y, 1/2; 1/2, y, 1/2 \pmod{n, n', n''};$   
 2 (a) 2  $0, y, 0; 1/2, y, 0 \pmod{n, n', n''}.$

La restriction à la seule répétition bidimensionnelle de translation donne les familles de Wyckoff de  $\mathcal{P}m2a$ , en remplaçant la lettre  $z$  par la lettre  $t$  pour rappeler le rôle particulier de la troisième coordonnée:

- 4 (d) 1  $x, y, t; \bar{x}, y, \bar{t}; 1/2 - x, y, t;$   
 $1/2 + x, y, \bar{t} \pmod{n, n', 0};$   
 2 (c) m  $1/4, y, t; 3/4, y, \bar{t} \pmod{n, n', 0};$   
 2 (a) 2  $0, y, 0; 1/2, y, 0 \pmod{n, n', 0}.$

On obtient les trois types de familles notés  $d, c, a$  issus des types de familles  $d, c, a$  de  $Pm2a$ ; on ne peut pas obtenir de familles issues du type  $b$  de  $Pm2a$  car ces positions sont toutes situées sur des axes binaires en dehors du plan  $\pi$ .

La méthode de Wood s'étend sans difficulté aux autres groupes de symétrie semi-cristallins (2+1)-dimensionnels: les résultats sont rappelés dans le Tableau 1 sous forme extrêmement condensée. La construction des familles de Wyckoff des groupes deux-colorés deux-dimensionnels n'offre aucune difficulté à partir des familles de Wyckoff des groupes de symétrie semi-cristallins (2+1)-dimensionnels, ainsi que nous l'avons montré dans § I. Les résultats figurent également dans le Tableau 1.

### III. Conclusion

Par le procédé que nous avons utilisé, on retrouve les quatre catégories de groupes colorés.

1ère catégorie: Groupes monoclores. Ces cristaux

ne comportent ni familles grises, ni familles incolores.

2ème catégorie: Groupes biclores vrais n'ayant pas de translation colorée. Cette catégorie de cristaux colorés possède des familles de positions unicolores et souvent des familles grises et des familles incolores.

3ème catégorie: Groupes biclores vrais ayant des translations colorées. Cette catégorie admet des familles de positions unicolores et souvent des familles grises et incolores.

4ème catégorie: Groupes gris. Ce type de cristaux colorés n'admet que des familles grises et incolores.

Il convient de remarquer qu'un groupe coloré contient autant de types de familles grises que de types de familles incolores puisqu'une famille incolore est la limite d'une famille grise quand les deux couleurs tendent l'une vers l'autre.

L'extension de ces concepts aux cristaux trois-dimensionnels deux-colorés n'offre pas de difficulté: ces cristaux sont les *projections cotées* de semi-cristaux (3+1)-dimensionnels qui s'étendent donc en dimension quatre de part et d'autre d'un hyperplan de dimension trois, la répétition périodique intervenant uniquement selon un groupe de translation trois-dimensionnel de cet hyperplan; on retrouve exactement les mêmes propriétés pour les familles de Wyckoff: familles de positions unicolores, grises et incolores.

### Références

- BELGUITH, J. (1980). Thèse de 3ème cycle, Tunis, Tunisie.  
 BELOV, N. V. & TARKHOVA, T. N. (1956). *Kristallografiya*, 1, 4-9.  
 BILLIET, Y., SAYARI, A. & ZARROUK, H. (1978). *Acta Cryst.* A34, 414-421, 811-819.  
 BILLIET, Y. & WEIGEL, D. (1981). *Acta Cryst.* A37, C348.  
*International Tables for X-ray Crystallography* (1952). Tome I. Birmingham: Kynoch Press.  
 JANNER, A. & ASCHER, E. (1963). *Cobalt Ions in Non-metallic Structures*. Tome II. Bruxelles: Centre d'Information du Cobalt.  
 WOOD, E. A. (1964a). *Bell Syst. Tech. J.* 43, 541-559.  
 WOOD, E. A. (1964b). *Bell Teleph. Syst. Tech. Pub. Monograph* No. 4680.

*Acta Cryst.* (1984). A40, 635-642

## A Retabulation of the 80 Layer Groups for Electron Diffraction Usage

By P. GOODMAN

CSIRO Division of Chemical Physics, PO Box 160, Clayton, Victoria, Australia 3168

(Received 17 June 1983; accepted 15 June 1984)

### Abstract

The 80 space groups of infinitely extended layers are identified as the defining groups for transmission electron diffraction symmetries obtained from lamellar crystals. These layer groups are retabulated using

a notation which characterizes the symmetries of convergent-beam diffraction patterns. The new tabulation provides a means for determining the three-dimensional space group of a particular structure from one or more convergent-beam zone-axis patterns. This is a two-stage process, involving

Table 1. Possible symmetry elements of a horizontal two-dimensionally-periodic layer

Symmetry elements for layer groups	Crystallographic symbols for symmetry elements	CBED symmetry operators
I. Vertical symmetry elements		I. Direct symmetries
1. Rotation axes of order 2, 3, 4, 6	2, 3, 4, 6,	Operators which leave crystal and incident and diffracted rays unchanged
2. Mirror planes	$m$ ,	
3. Glide planes with horizontal translational components	$a, b$	
II. Horizontal symmetry elements located on the central plane		II. Indirect symmetries
1. Diad axes	2,	Operators which invert the crystal and introduce symmetries through reciprocity.
2. Two-fold screw axes	$2_1$ ,	
3. Mirror plane	$m$ ,	
4. Glide plane with horizontal translational component	$g$ ( $a, b$ , or $n$ )	
5. Centre of inversion	$\bar{1}$	
6. Vertical tetrad inversion axis	$\bar{4}$	I and II: $\bar{4}$ combines direct and indirect symmetries

determination of a layer-group corresponding to a principal zone-axis pattern, followed by identification, where necessary, of the appropriate class-equivalent subgroup. For this final identification, the three-dimensional extinction conditions, determined from an alternative set of convergent-beam zone-axis patterns, are required. In terms of standard group symbols [e.g. Vainshtein (1981). *Modern Crystallography I*. Berlin: Springer], the one-way interrelation between patterns and space groups  $G_2^3 \rightarrow G_3^3$  (space group analysis) is given. The inverse problem, equally accessible from group theory, of providing the interrelation  $G_3^3 \rightarrow G_2^3$  (pattern symmetry prediction) is left for separate tabulation.

### 1. Introduction

The 80 space groups of parallel-sided layers, first derived by Alexander & Hermann (1929), describe the possible symmetry arrangements for two-dimensionally infinite one-dimensionally finite sheets which have periodic arrangement in only two dimensions; they are therefore known as 'partially periodic' groups (see for example Shubnikov & Kopstik, 1974; Vainshtein, 1981). The groups are formed by combining the 17 groups of an  $x$ - $y$  plane at  $z = 0$  with certain three-dimensional symmetry elements, namely  $m$ ,  $g$ , 2,  $2_1$ ,  $\bar{1}$  and  $\bar{4}$  [*International Tables for X-ray Crystallography* (IT) symbols], located in the horizontal plane  $z = 0$ , which provides additional symmetry relations between the  $+z$  and  $-z$  sides of the plane. These two categories of symmetry elements ('vertical' and 'horizontal' with respect to the layer), are given in Table 1.

Recently, we have found the 80 Alexander & Hermann groups to be the defining groups for transmission electron diffraction symmetries obtained from lamellar crystals (Goodman, 1984). Comparison of the elements of these groups with those obtained independently for convergent-beam electron diffrac-

tion (CBED) patterns (see for example Tanaka, Saito & Sekii, 1983), as shown in Table 1, offers sufficient proof that this is correct. In CBED terminology the categories of Table 1 correspond to 'direct' and 'indirect' (or reciprocity-related) symmetry elements, with the complication that  $\bar{4}$  is not purely one or the other since it combines direct (a  $z$ -directed rotation axis) with indirect (centro-inversionary) symmetry operations.

The first group treatment of these symmetries was given by Buxton, Eades, Steeds & Rackham (1976). By identifying reciprocity with colour reversal they obtained 31 'diffraction groups', isomorphous with the 31 Shubnikov (1964) groups for plane figures. Buxton *et al.* gave a space-group-determination procedure in which identification of crystallographic point group was made through association with the 'diffraction group' of the pattern. However, the subsequent determination of a space group has, until now, required identification of absences and  $hk0$  extinctions as a separate exercise.

### 2. Tabulation

In the present tabulation we identify the 31 BESR (Buxton, Eades, Steeds & Rackham) groups, listed in column 4 of Table 2, as the point-group component of the original Alexander & Hermann space groups. These latter then provide us with an 80-member classification system for CBED patterns which includes the main extinction characteristics, and from which the identification of space group is relatively straightforward. We endeavour in Table 2 to give a logical space-group ordering, and an explicit group nomenclature, so that the space-group symbols for  $G_2^3$  (Vainshtein, 1981)\* serve both to identify the

\* We have adopted Vainshtein's notation for partially periodic groups,  $G_n^r$ , where  $n$  gives the dimensionality of the space in which the group is defined and  $r$  the dimensionality of the periodic lattice component.

Table 2. Tabulation of the 80 members of the layer space-group system  $G_2^3$  together with the interrelating members of the three-dimensional space-group system  $G_3^3$ 

The code for the subheadings is as follows: S-K No. refers to the group-number system given by Shubnikov & Kopstik (1974); H-M refers to the Hermann-Mauguin nomenclature;  $\varphi_s$ ,  $\varphi_n$ , and  $\varphi_a$  are the symmorphic, non-symmorphic and asymmorphic subdivisions of the space groups, respectively.

System		80 $G_2^3$							230 $G_3^3$
S-K		Point group	BESR	Space group		Proposed			System
No.	No.	H-M		$\varphi_s$	$\varphi_n$	$\varphi_s$	$\varphi_n$	$\varphi_a$	Space group
		IT Nos.							
Oblique		Triclinic							
1	1	1	1	$P1$		$P1$			1
2	3	$\bar{1}$	$2_R$	$P\bar{1}$		$P\bar{1}$			2
3	5	12	2	$P112$		$P2$			3 <sup>4</sup> , 4 <sup>4</sup> , 5 <sup>4</sup>
4	2	$1m$	$1_R$	$P11m$		$P1, m$			6 <sup>4</sup> , 8 <sup>4</sup>
5	4	$1m$	$1_R$		$P11b$			$P1, b$	7 <sup>4</sup> , 9 <sup>4</sup>
6	6	$2/m$	$21_R$	$P112/m$		$\bar{P}2, m$			10 <sup>4</sup> , 11 <sup>4</sup> , 12 <sup>4</sup>
7	7	$2/m$	$21_R$		$P112/b$			$\bar{P}2, b$	13 <sup>4</sup> , 14 <sup>4</sup> , 15 <sup>4</sup>
Rectangular		Orthorhombic							
8	14	21	$m_R$	$P121$		$P1, 2$			3, 5 <sup>2</sup>
9	15	21	$m_R$		$P12, 1$		$P1, 2_1$		4
10	16	21	$m_R$	$C121$		$C1, 2$			5
11	8	$m1$	$m$	$P1m1$		$Pm$			6 <sup>2</sup> , 7, 8 <sup>2</sup>
12	10	$m1$	$m$		$P1a1$		$Pa$		7 <sup>2</sup> , 9 <sup>2</sup>
13	12	$m1$	$m$	$C1m1$		$Cm$			8, 9
14	17	$12/m$	$2_Rmm_R$	$P12/m1$		$\bar{P}m, 2$			10, 13, 12 <sup>2</sup>
15	18	$12/m$	$2_Rmm_R$		$P12, /m1$		$\bar{P}m, 2_1$		11, 14
16	20	$12/m$	$2_Rmm_R$		$P12/a1$		$\bar{P}a, 2$		13 <sup>2</sup> , 15 <sup>2</sup>
17	21	$12/m$	$2_Rmm_R$		$P12/a$		$\bar{P}a, 2_1$		14 <sup>2</sup>
18	19	$12/m$	$2_Rmm_R$	$C12/m1$		$\bar{C}m, 2$			12, 15
19	37	222	$2m_Rm_R$	$P222$		$P2, 22$			16, 17, 21, 22: <u>195, 196</u>
20	38	222	$2m_Rm_R$		$P2, 22$		$P2, 2, 2$		17 <sup>3</sup> , 18 <sup>2</sup> : 20 <sup>3</sup>
21	39	222	$2m_Rm_R$		$P2, 2, 2$		$P2, 2, 2_1$		18, 19: <u>198</u>
22	40	222	$2m_Rm_R$	$C222$		$C2, 22$			21, 20, 23, 24: <u>197, 199</u>
23	22	$mm2$	$2mm$	$Pmm2$		$P2mm$			25, 26, 27: 38, 39, 42
24	24	$mm2$	$2mm$		$Pbm2$		$P2mb$		28, 29 <sup>3</sup> , 30, 31 <sup>3</sup> : 40, 41
25	26	$mm2$	$2mm$		$Pba2$		$P2ab$		32, 33, 34: 43
26	28	$mm2$	$2mm$	$Cmm2$		$C2mm$			35, 36, 37: 44, 45, 46
27	9	$2mm$	$m1_R$	$P2mm$		$Pm, 2m$			25 <sup>3</sup> , 28 <sup>4</sup> : 35 <sup>3</sup> , 42 <sup>3</sup>
28	11	$2mm$	$m1_R$		$P2, am$		$Pa, 2, m$		26 <sup>3</sup> , 31 <sup>4</sup>
29	33	$2mm$	$m1_R$		$P2, ab$		$Pa, 2, b$		29 <sup>3</sup> , 33 <sup>3</sup>
30	30	$2mm$	$m1_R$		$P2, ma$			$Pm, 2, a$	26 <sup>3</sup> , 29 <sup>4</sup> : 36 <sup>3</sup>
31	35	$2mm$	$m1_R$		$P2, mn$			$Pm, 2, n$	31 <sup>3</sup> , 33 <sup>5</sup>
32	32	$2mm$	$m1_R$		$P2mb$			$Pm, 2b$	28 <sup>6</sup> , 32 <sup>5</sup> , 40 <sup>3</sup>
33	31	$2mm$	$m1_R$		$P2aa$			$Pa, 2a$	27 <sup>3</sup> , 30 <sup>3</sup> : 37 <sup>3</sup>
34	34	$2mm$	$m1_R$		$P2an$			$Pa, 2n$	30 <sup>4</sup> , 34 <sup>3</sup> : 43 <sup>3</sup>
35	13	$2mm$	$m1_R$	$C2mm$		$Cm, 2m$			38 <sup>4</sup> , 40 <sup>4</sup> , 44 <sup>3</sup> , 46 <sup>4</sup>
36	36	$2mm$	$m1_R$		$C2mb$			$Cm, 2b$	39 <sup>4</sup> , 41 <sup>4</sup> , 45 <sup>3</sup> , 46 <sup>3</sup>
37	23	$mmm$	$2mm1_R$	$Pmmm$		$\bar{P}2mm, m$			47, 49, 51 <sup>5</sup> : 65 <sup>4</sup> , 67 <sup>3</sup> , 69: <u>200, 202</u>
38	25	$mmm$	$2mm1_R$		$Pbma$		$\bar{P}2mb, 2, m$		51 <sup>3</sup> , 53 <sup>3</sup> , 57, 59 <sup>3</sup> : 63 <sup>3</sup> , 64 <sup>2</sup>
39	27	$mmm$	$2mm1_R$		$Pbam$		$\bar{P}2ab, 2, m$		55, 58, 62 <sup>6</sup>
40	46	$mmm$	$2mm1_R$		$Pamb$		$\bar{P}2am, 2, b$		57 <sup>4</sup> , 60 <sup>5</sup> , 61 <sup>2</sup> , 62 <sup>2</sup> : <u>205</u>
41	45	$mmm$	$2mm1_R$		$Pbaa$		$\bar{P}2ba, 2, a$		54 <sup>3</sup> , 52, 56 <sup>3</sup> , 60 <sup>5</sup>
42	43	$mmm$	$2mm1_R$		$Pmma$			$\bar{P}2mm, a$	51, 54, 55 <sup>5</sup> , 57 <sup>3</sup> : 63 <sup>3</sup> , 64 <sup>3</sup>
43	47	$mmm$	$2mm1_R$		$Pmnn$			$\bar{P}2mm, n$	59, 56, 62 <sup>4</sup>
44	44	$mmm$	$2mm1_R$		$Pbmn$			$\bar{P}2mb, n$	53 <sup>3</sup> , 52 <sup>3</sup> , 58 <sup>5</sup> , 60
45	41	$mmm$	$2mm1_R$		$Pmaa$			$\bar{P}2am, a$	49 <sup>3</sup> , 50 <sup>3</sup> , 53, 54 <sup>4</sup> : 66 <sup>3</sup> , 68 <sup>4</sup>
46	42	$mmm$	$2mm1_R$		$Pban$			$\bar{P}2ab, n$	50, 52 <sup>3</sup> , 48, 70: <u>201, 203</u>
47	29	$mmm$	$2mm1_R$	$Cmmm$		$\bar{C}2mm, m$			65, 63, 66, 72, 74 <sup>3</sup> , 71: <u>204</u>
48	48	$mmm$	$2mm1_R$		$Cmma$			$\bar{C}2mm, a$	67, 64, 68: 72 <sup>5</sup> , 74, 73: <u>206</u>

group and to describe the predicted CBED pattern character.

Hall (1981) introduced an explicit matrix-based nomenclature for the 230 space groups of  $G_3^3$ , definitive in both real and reciprocal space. Although we are following Hall's basic ideas in using matrix-based symmetry symbols, our application differs from Hall's in several ways. Firstly, we are interested in characterizing a diffraction pattern rather than a unit-cell origin, which helps to simplify the nomenclature. Furthermore, there is an additional need to separate 'direct' and 'indirect' symmetry element symbols. This is done in columns 7 to 9 of Table 2, headed 'proposed symbols', by the use of a comma (,) to separate these

categories, with direct elements coming before the comma. Groups having only direct symmetries have no comma in the symbol and therefore have a symbol identical to the Hermann-Mauguin symbol in columns 5 and 6 of Table 2; they represent the monochromatic or 'black' groups in colour-group nomenclature. In addition we have adopted two of Hall's symbols, namely a bar above the lattice symbol (as in  $\bar{P}$  and  $\bar{C}$ ) to indicate centrosymmetry and primed symbols (as in  $m''$  and  $2''$ ) to indicate diagonal as distinct from axial settings of specific elements. Since our main aim is to characterize diffraction groups, the primed symbols above are always used to indicate a diagonal setting in *diffraction* space coordinates. This

Table 2 (cont.)

System		80 $G_2^3$						230 $G_3^3$	
		Point group	BESR	Space group		Proposed			System
S-K	H-M			$\varphi_s$	$\varphi_n$	$\varphi_s$	$\varphi_n$	$\varphi_a$	Space group
No.	No.								IT Nos.
Square									
49	50	4	4	$P4$		$P4$			Tetragonal
50	51	$4/m$	$41_R$	$P4/m$		$\bar{P}4, m$			75 77, 76, 78; 79, 80
51	57	$4/m$	$41_R$		$P4/n$			$\bar{P}4, n$	83 84; 87
52	55	422	$4m_R m_R$	$P422$		$P4, 22''$			85 86, 88
53	56	422	$4m_R m_R$		$P42, 2$		$P4, 2, 2''$		89 93, 91, 95; 97, 98:
54	52	$4mm$	$4mm$	$P4mm$		$P4mm''$			<u>207, 208, 209, 210; 211, 214</u>
55	59	$4mm$	$4mm$		$P4bm$		$P4abm''$		90 94, 92, 96; 212, 213
56	53	$4/mmm$	$4mm1_R$	$P4/mmm$		$\bar{P}4mm'', m$			99 101, 103, 105; 107, 108
57	58	$4/mmm$	$4mm1_R$		$P4/mbm$		$\bar{P}4m''ab, 2, 1m$		100 102, 104, 106; 109, 110
58	62	$4/mmm$	$4mm1_R$		$P4mbn$			$\bar{P}4m''ab, 2n$	123 124, 131, 132; 139, 140:
59	63	$4/mmm$	$4mm1_R$		$P4/nmm$			$\bar{P}4mm'', 2, n$	<u>221, 223; 225, 226; 229</u>
60	49	$\bar{4}$	$4_R$	$P\bar{4}$		$P\bar{4}$			127 128, 135, 136
61	61	$\bar{4}2m$	$4_R mm_R$	$P\bar{4}m2$		$P\bar{4}m, 2''$			125 126, 133, 134; 141, 142:
62	64	$\bar{4}2m$	$4_R mm_R$		$P\bar{4}b2$		$P\bar{4}ab, 2''$		<u>222, 224; 227, 228; 230</u>
63	54	$\bar{4}2m$	$4_R mm_R$	$P\bar{4}2m$		$P\bar{4}m'', 2$			129 130, 137, 138
64	60	$\bar{4}2m$	$4_R mm_R$		$P\bar{4}2, m$		$P\bar{4}m'', 2, 1$		81 82
65	65	3	3	$P3$		$P3$			115 116; 119, 120
66	67	$\bar{3}$	$6_R$	$P\bar{3}$		$P\bar{3}$			117 118; 122; <u>220</u>
67	72	32	$3m_R$	$P312$		$P3, 2$			111 112; 121:
68	73	32	$3m_R$	$P321$		$P3, 2''$			<u>215, 216, 217, 218, 219</u>
69	70	$3m$	$3m$	$P31m$		$P3m''$			113 114
70	68	$3m$	$3m$	$P3m1$		$P3m$			Trigonal
71	74	$6mm$	$6_R mm_R$	$P\bar{3}1m$		$\bar{P}3m'', 2$			143 144, 145; 146
72	75	$6mm$	$6_R mm_R$	$P\bar{3}m1$		$P3m, 2''$			147 148
73	76	6	6	$P6$		$P6, 22''$			149 151, 153
74	66	$\bar{6}$	$31_R$	$P\bar{6}$		$P6mm''$			150 152, 154; 155
75	80	622	$6m_R m_R$	$P622$		$\bar{P}6, m$			157 159
76	78	$6mm$	$6mm$	$P6mm$		$P6m''$			156 158; 160, 161
77	77	$6/m$	$61_R$	$P6/m$		$\bar{P}6m'', 22''m$			162 163
78	79	$6/mmm$	$6mm1_R$	$P6/mmm$		$P3m'', 2''m$			164 165; 166, 167
79	71	$6m2$	$3m1_R$	$P62m$		$P3m, 2m$			Hexagonal
80	69	$6m2$	$3m1_R$	$P6m2$					168 171, 172, 173, 169, 170

additional clarification is needed in the hexagonal system. Otherwise, the symmetry elements have their standard international crystallographic meaning as  $3 \times 3$  matrix operators.

The symbols given in columns 7 to 9 have the advantage that they can be interpreted simply in terms of CBED pattern symmetries.\* This advantage continues beyond the symmorphic group listing,  $\varphi_s$ , (of 43 groups) of column 7. The classification system leads naturally to a further subdivision of the remaining 37 groups into 'non-symmorphic' and 'asymmorphic' components, recognizable from the group symbol. The first of these,  $\varphi_n$ , refers to groups which give extinctions [Gjønnes-Moodie (1965) bands] in the space-group-forbidden reflexions visible in the zero-layer pattern. The second category,  $\varphi_a$ , listed in column 9, refers to those groups giving rise to patterns that, to the first order in observables, are simply centred or halved in  $a$  or  $b$ ; Gjønnes-Moodie bands then only occur through upper-layer interactions and are generally too weak to identify (see,

\* This follows from the existence of a simple coordinate transformation between crystal and CBED pattern space (Goodman, 1984). It is not necessary, however, to have these transformations in order to visualize the corresponding CBED pattern symmetries.

however, Ishizuka & Taftø, 1982). In the simplest example of this,  $a$  in groups 16 and 17 will give extinction bands parallel to the  $a$  translation, while  $b$  in groups 5 and 7 will lead (to a first approximation) to a halving of the  $b$  axis (or a doubling of the  $b^*$  axis).†

$\varphi_a$  groups may be identified, without reference to experimental conditions, as those groups possessing a horizontal glide (' $a$ ', ' $b$ ' or ' $n$ ') and having no non-primitive translations *additional* to those given by this defining element.

(i) *Directly related space groups: column 10*

The Hermann-Mauguin symbols for the layer groups (Holser, 1958) have been retained in parallel tabulation in columns 5 and 6, since they give a direct lead to the listings in *International Tables for X-ray Crystallography* (1965) and *International Tables for Crystallography* (1983). Column 10 of Table 2 (the first column after the dividing line between  $G_2^3$  and  $G_3^3$ ) gives the IT number of the three-dimensional space group from which the particular layer group is

† In the notation adopted by Tanaka, Sekii & Nagasawa (1983), these extinctions are GM bands of types  $A_2$  and  $A_3$ , respectively.

Table 3. Layer-equivalent subgroups of space groups in  $G_3^3$  for *Pmab* (no. 57) and *Pbaa* (no. 54)

IT no.	Full H-M symbol	$0kl$	$h0l$	$hk0$	$h00$	$0k0$	$00l$
	$\bar{P}2am, 2_1b$						
57 <sup>4</sup>	$\frac{2_1}{m} \frac{2_1}{a} \frac{2}{b}$		$h = 2n$	$k = 2n$	$h = 2n$	$k = 2n$	
60 <sup>6</sup>	$\frac{2_1}{c} \frac{2_1}{n} \frac{2}{b}$	$l = 2n$	$h + l = 2n$	$k = 2n$	$h = 2n$	$k = 2n$	
61 <sup>2</sup>	$\frac{2_1}{c} \frac{2_1}{a} \frac{2_1}{b}$	$l = 2n$	$h = 2n$	$k = 2n$	$h = 2n$	$k = 2n$	$l = 2n$
62 <sup>2</sup>	$\frac{2_1}{m} \frac{2_1}{n} \frac{2_1}{b}$		$h + l = 2n$	$k = 2n$	$h = 2n$	$k = 2n$	$l = 2n$
	$\bar{P}2ab, 2_1a$						
54 <sup>3</sup>	$\frac{2}{b} \frac{2_1}{a} \frac{2}{a}$	$k = 2n$	$h = 2n$	$h + k = 2n$		$k = 2n$	
52	$\frac{2}{n} \frac{2_1}{n} \frac{2}{a}$	$k + l = 2n$	$h + l = 2n$	$h = 2n$		$k = 2n$	
56 <sup>3</sup>	$\frac{2}{n} \frac{2_1}{a} \frac{2_1}{a}$	$k + l = 2n$	$h = 2n$	$h = 2n$		$k = 2n$	$l = 2n$
60 <sup>5</sup>	$\frac{2}{b} \frac{2_1}{n} \frac{2_1}{a}$	$k = 2n$	$h + l = 2n$	$h = 2n$		$k = 2n$	$l = 2n$

sectioned (*i.e.* derived by suppression of the primitive,  $z$ , translation), which therefore has the same Hermann–Mauguin symbol (as that given in columns 5 and 6).

Although IT Vol. A has retained the ordering number for space groups of earlier volumes, the ordering of *settings* has been changed. Hence, in giving the entries of column 10 a numerical superscript (as in 26<sup>5</sup> and 26<sup>3</sup>) to denote a non-standard setting, the scheme of the later IT Vol. A has been used. This superscripted number then corresponds to the column number given in Table 4.3.1 to that volume.

In some cases, alternate settings of the same IT space group occur on different rows of Table 2. Hence, nine entries in column 10 are generated by a multiple listing of the same member of  $G_3^3$  in alternate settings. Therefore there are  $80 - 9 = 71$  distinct space groups interrelated directly with the 80 layer groups in Table 2.

It is important to note that the methodology of Table 2 relates initially to a *principle* or maximal-symmetry zone-axis setting of a crystal in a particular three-dimensional system. This has a unique meaning in the tetragonal and hexagonal systems (which will be obvious from the table), and the same is true for the cubic system, but for the monoclinic and orthorhombic systems there are three equally valid choices for a principal setting leading, generally, to three distinct layer-group indexations.

### (ii) Subgroup expansion: column 11

In order to relate individual layer groups to all 230 space groups, it is necessary to expand from those specific groups entered in column 10, by means of subgroup relationships, to the remainder. This means including groups which are subgroups of the same

class in  $G_3^3$ , and in particular those subgroups which are not also subgroups in  $G_2^3$  and hence already listed separately in the table. These additional groups, appearing as rows of space-group numbers in column 11 of Table 2, are referred to as 'layer-equivalent' subgroups, one specific example of their derivation being given in Table 3. They correspond, collectively, to an exhaustive listing of maximal subgroups of type IIb (IT Vol. A), and permit access to all non-cubic groups. Further extension, to general subgroups which include suppression of the defining trigonal point-group elements, is required to include the cubic space groups. These are included in the rows of Table 2 in an extension within column 11 as numbers which are underlined.

In this way, Table 2 provides a complete theoretical link between the 80 groups of  $G_2^3$  and the 230 groups of  $G_3^3$ .

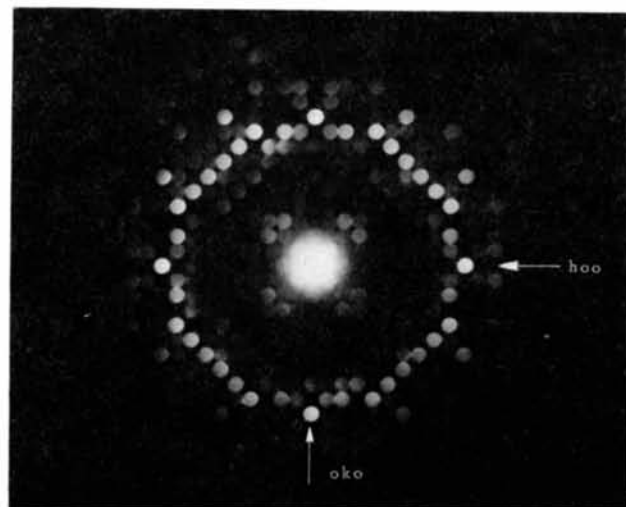
## 3. Application and discussion

Identification of a crystallographic space group from a CBED pattern using Table 2 is therefore a two-stage procedure following (i) and (ii) above, which is best explained by means of examples. These have been chosen from large-unit-cell structures, which are not commonly used in illustration of CBED analysis. However, the current procedure, which is as dependent upon identification of characteristic extinctions as upon determining symmetries between reflexions, works quite as well for these cases as for the more commonly illustrated small-unit-cell structures. The tetragonal and orthorhombic examples given allow the application to be demonstrated in those regions of the three-dimensional space-group tables where the greatest complexity of non-symmorphic expansion exists.

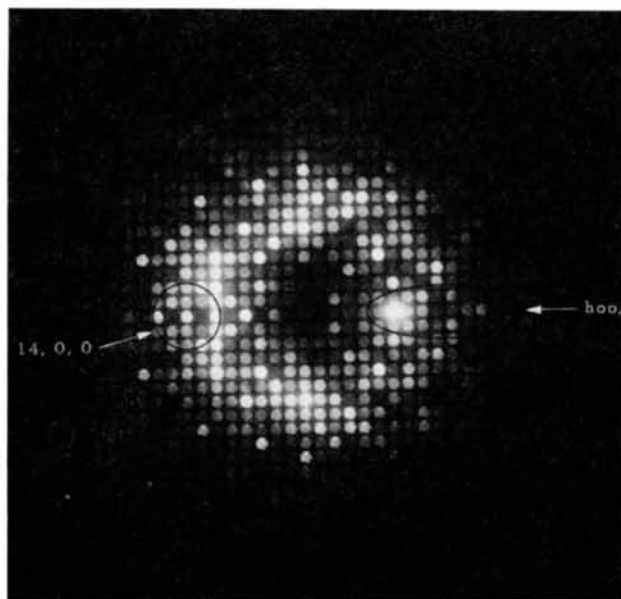
(1) *Tetragonal structure*:  $\text{Rb}_{22}\text{Nb}_{54}\text{O}_{146}$  ( $a = 27.5$ ,  $b = 4.0 \text{ \AA}$ ). Fig. 1(a) shows a zone-axis pattern from this structure, which is discussed in more detail elsewhere (Olsen, McLean & Goodman, 1983). Since it has fourfold axial symmetry it belongs to the square system of  $G_2^3$ . Further, since it shows extinctions corresponding to  $h00$ ,  $h = 2n$  ( $0k0$ ,  $k = 2n$ ), it belongs to the  $\varphi_n$  classification of column 8, with the characterizer  $4ab$  in the space-group symbol. Fig. 1(b), for which the crystal is rotated away from the [001] zone axis, shows that only those  $h00$  reflexions very close to the Laue circle are extinguished; those near the 000 reflexion have strong intensity. This is an indication, according to the literal interpretation of the Gjønnes–Moodie (1965) rules (and later supported by the other zone-axis patterns of Fig. 2), that the horizontal screw axis  $2_1$  parallel to  $a^*$  is present in addition to the vertical glide planes. This observation permits only one layer-group indexation, namely no. 57 or  $\bar{P}4m''ab, 2_1m$ . The space group in  $G_3^3$  (directly linked to no. 57 in  $G_2^3$ ) is no. 127, or  $p4/mbm$ . For

this space group there are three relevant subgroups (not already entered as alternative layer groups), namely nos. 128, 135 and 136, which are listed in column 11 of Table 2. These four groups can be distinguished by means of their extinction conditions for  $0kl$  and  $hhl$  reflexions. Figs. 2(a) and (b) show the alternative zone axes  $[0\bar{1}1]$  and  $[0\bar{1}4]$ , respectively, for the same structure. From these CBED patterns we see that the  $011$  reflexion is extinguished but that

the  $041$  reflexion is present and of medium strength. This establishes the  $0kl$  condition as  $k = 2n$  and rules out the alternative condition  $k + 1 = 2n$ . Next, it can be seen that the reflexions  $111$  and  $\bar{1}\bar{1}1$ , neighbouring the arrowed  $011$  reflexion in Fig. 2(a), are strong. This second observation, on  $hhl$ -type reflexions, establishes that they are 'allowed' (i.e.  $hhl$ : 'no conditions'). These observations eliminate nos. 128, 135 and 136 as possibilities, and confirm no. 127 as the

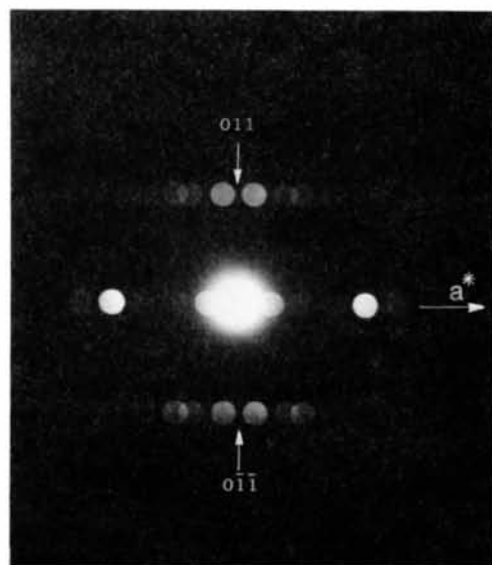


(a)

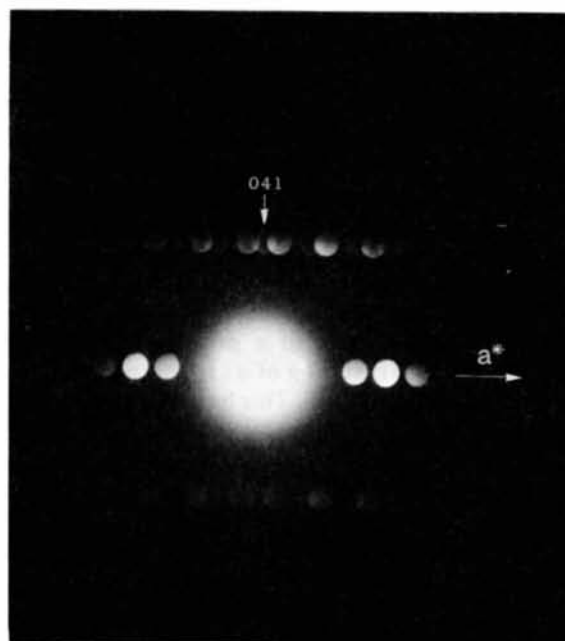


(b)

Fig. 1. (a)  $[001]$  zone-axis pattern from  $\text{Rb}_{22}\text{Nb}_{54}\text{O}_{146}$ , showing fourfold symmetry and the systematic extinctions  $h00$   $h = 2n + 1$ ,  $k00$   $k = 2n + 1$ . (b) Pattern taken from the same region as in (a), but with the crystal rotated from the exact zone-axis setting. The centre of the Laue circle is marked with a cross. At this tilt: (i) the  $h00$  reflexions, which are identified by an enclosing ellipse, are all present; (ii) the  $h00$  reflexions neighbouring the strong  $12,0,0$  and  $14,0,0$  reflexions and enclosed with a labelled circle are extinguished.



(a)



(b)

Fig. 2.  $[0\bar{1}1]$  and  $[0\bar{1}4]$  zone-axis patterns from  $\text{Rb}_{22}\text{Nb}_{54}\text{O}_{146}$ , showing (a)  $011$ ,  $0\bar{1}\bar{1}$  reflexions extinguished and (b)  $041$  reflexion present. Note that the spacing of discs along the  $a^*$  line in (a) and (b) is halved, in accordance with the rule  $h00$ :  $h = 2n$ .

correct space group. The confirmatory evidence of the symmetry element  $2_1$ , parallel to  $a^*$ , referred to above, is found in Figs. 2(a) and (b), since all  $h00$ -type reflexions,  $h = 2n + 1$ , are absent (this is evident along the  $a^*$  lines of the figures).

(2) *Orthorhombic structure*:  $\text{Cu}_3\text{SbSe}_3$  ( $a = 10.22$ ,  $b = 7.84$ ,  $c = 6.60 \text{ \AA}$ ). The type of CBED pattern shown in Fig. 3, belonging to the rectangular system, which contains extinction bands along the  $a^*$  axis ( $h = 2n$  for  $h00$ ) and also has every alternate line extinguished along  $b^*$  ( $k = 2n$  for  $hk0$ ; this is evident in tilted point patterns of the type shown in Fig. 3(b)), implies a non-symmorphic, column 8, layer-group index  $\varphi_n$  for this structure of either 40 ( $\overline{P}2am, b$ ) or 41 ( $\overline{P}2ba, b$ ). Without additional data it is not possible to distinguish between these layer groups without

going through the same work as is needed to distinguish between the subgroups in  $G_3^3$  (listed in column 11). Thus, the IT space groups listed in row 40 are 57, 60, 61, 62 (ignoring the underlined group 205 from the cubic system, which is not a possibility here) and those in row 41 are 54, 52, 56, 60 (all in appropriate settings).

Table 3 lists the layer-equivalent subgroups of  $Pmab$  (no. 40) and  $Pbaa$  (no. 41) and serves to illustrate the way in which these are derived. Column 2 of Table 3 gives the full H-M symbol for the space group in the appropriate setting (defined by the superscripted number in column 1). Columns 3 to 9 give the appropriate three-dimensional extinction conditions, collated from the appropriate pages of IT. Inspection of this part of the table shows that each group is distinctively identified, even when the last, or  $00l$  condition (generally inaccessible to a principle orientation, by definition), is excluded.

In this particular case, 62 could be decided as the correct space group since the single upper-layer diffraction condition found from additional diffraction data was  $h0l$ ,  $h + l = 2n$  (Whitfield, private communication).

#### 4. Additional comments on the proposed symbols

Since the symbols given in columns 7 to 9 of Table 2 are proposed ones only, some modifications may be found desirable after some use, but the following additional comments suggest themselves. We have not tried to give a minimum set of elements, but rather to give a sufficient number for identification purposes, and approximately in order of importance for CBED identification. Centrosymmetry, for example, which is a very important property for CBED work, is immediately indicated. On the other hand, use of the prime (') to indicate diagonal setting would lead to confusion since it is used in Shubnikov's nomenclature to indicate formal anti-symmetry; hence the alternative Hall double prime (") is better, though it is never possible to avoid overlapping some other nomenclature in some respect. With respect to the explicit distinction between direct and indirect operators, the alternative of using subscripts  $v$  and  $h$  on the symmetry symbols, as is commonly done in the Schoenflies space-group symbols, to represent the vertical and horizontal elements was also considered, but the present proposal was finally adopted for reasons of compactness, and ease of hand writing and type-setting. Finally, a shortened version of these symbols, which may well prove the more usable, is readily derivable from the fully-descriptive symbols listed.

The author wishes to thank A. F. Moodie and H. Whitfield for suggesting the use of Fig. 3, from their recent work (Moodie & Whitfield, 1984), as an

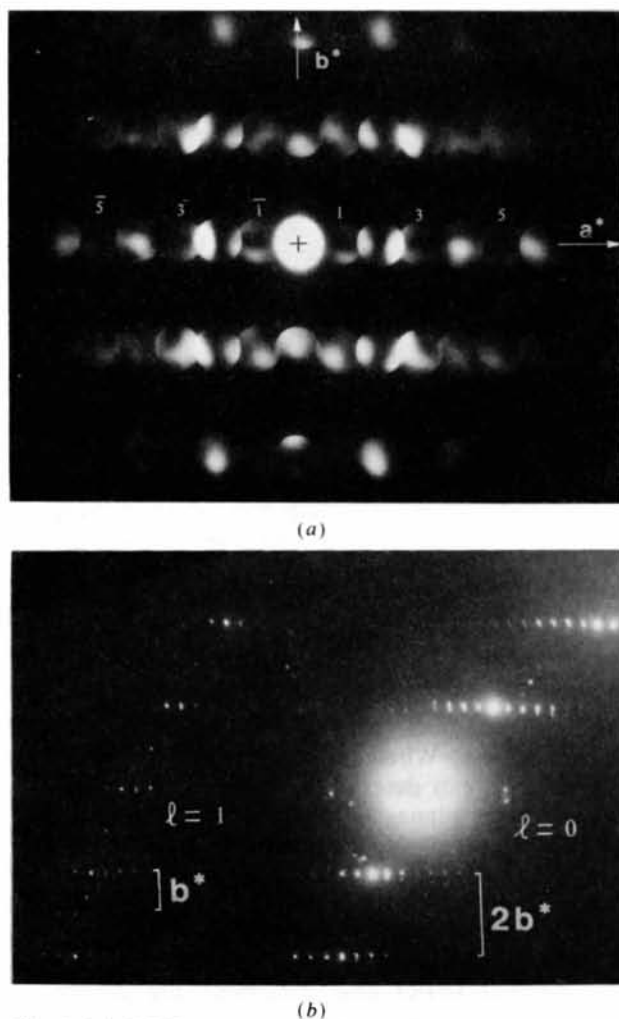


Fig. 3. (a) CBED pattern, taken in the JEOL 200CX top-entry stage (condensor-focused probe), from the  $[001]$  zone axis of  $\text{Ge}_3\text{SbSe}_3$ , showing extinction bands along the  $a^*$  axis in the odd-order reflexion discs indicated (see text for Moodie & Whitfield reference). (b) A tilted point diffraction pattern taken so as to show parts of both the zero- and first upper-layer reflexion zones. Additional lines appearing in the first upper-layer zone demonstrate that  $b^*$  is halved in the zero-layer pattern (see text).

illustration. Helpful discussions with A. Olsen on possible space-group-symbol arrangements are also gratefully acknowledged. Finally, I am indebted to Drs A. F. Moodie, A. W. S. Johnson, A. C. Hurley and Professor Dr Th. Hahn for their collective careful and critical reading of the original manuscript.

#### References

ALEXANDER, E. & HERMANN, K. (1929). *Z. Kristallogr.* **70**, 328–345.  
 BUXTON, B. F., EADES, J. A., STEEDS, J. W. & RACKHAM, G. M. (1976). *Philos. Trans. R. Soc. London*, **281**, 171–194.  
 GJØNNES, J. & MOODIE, A. F. (1965). *Acta Cryst.* **19**, 65–67.  
 GOODMAN, P. (1984). *Acta Cryst.* **A40**, 522–526.  
 HALL, S. R. (1981). *Acta Cryst.* **A37**, 517–525.  
 HOLSER, W. T. (1958). *Z. Kristallogr.* **110**, 266–281.  
*International Tables for Crystallography* (1983). Vol. A, edited by TH. HAHN. Dordrecht: Reidel.

*International Tables for X-ray Crystallography* (1965). Vol. 1. Birmingham: Kynoch Press.  
 ISHIZUKA, K. & TAFTØ, J. (1982). *Proceedings of the 40th. Annual Meeting: Electron Microscopic Society of America*. New York: Claitor.  
 MOODIE, A. F. & WHITFIELD, H. J. (1984). *Ultramicroscopy*, **13**, in the press.  
 OLSEN, A., MCLEAN, J. D. & GOODMAN, P. (1983). *Proceedings of the 41st. Annual Meeting: Electron Microscopic Society of America*. New York: Claitor.  
 SHUBNIKOV, A. V. (1964). *Coloured Symmetry*, edited by W. T. HOLSER. Oxford: Pergamon Press.  
 SHUBNIKOV, A. V. & KOPSTIK, V. A. (1974). *Symmetry in Science and Art*. New York: Plenum Press.  
 TANAKA, M., SAITO, R. & SEKII, H. (1983). *Acta Cryst.* **A39**, 357–368.  
 TANAKA, M., SEKII, H. & NAGASAWA, T. (1983). *Acta Cryst.* **A39**, 825–837; *erratum: Acta Cryst.* (1984), **A40**, 721.  
 VAINSHTEIN, B. K. (1981). *Modern Crystallography* I. Berlin: Springer-Verlag.

*Acta Cryst.* (1984). **A40**, 642–645

## Orientation Relationships Between Two Crystal Lattices: Matrix Description

BY M. A. FORTES

*Departamento de Metalurgia, Instituto Superior Técnico; Centro de Mecânica e Materials da Universidade Técnica de Lisboa (CEMUL), Avenue Rovisco Pais, 1096 Lisboa CODEX, Portugal*

(Received 13 April 1984; accepted 3 May 1984)

#### Abstract

Orientation relationships between two crystal lattices are frequently specified in terms of parallel directions and planes in each lattice. The corresponding matrix, relating the vector bases of the lattices, can be obtained by a general method involving the metric matrices of the two lattices and the crystallographic indices of parallel planes and directions. Equivalent matrices can be defined by changing the lattice bases: different selections of the invariants of such matrices are indicated. Finally, criteria for choosing the 'best' matrix relating the two lattices are discussed in the context of phase transformations and of interfacial structure.

#### 1. Introduction

There are various situations where it is of interest to specify the relative orientation of two crystal lattices; for example, when the two crystals meet at an interface or when one of the crystals is phase transformed into the other. Frequently, the relative orientation is defined by indicating the crystallographic indices of planes or directions, in each lattice, that are parallel to each other. The possibilities are: two pairs of parallel directions; two pairs of parallel planes; one pair of directions and one pair of planes, this being

the more commonly used. However, the most convenient and formally simpler way of specifying the relative orientation of two lattices with bases  $(\mathbf{e}_1, \mathbf{e}_2, \mathbf{e}_3) \equiv (\mathbf{e})$  and  $(\mathbf{e}'_1, \mathbf{e}'_2, \mathbf{e}'_3) \equiv (\mathbf{e}')$ , respectively, is in terms of the  $3 \times 3$  matrix  $X$  that relates the two bases:

$$[\mathbf{e}'_1 \ \mathbf{e}'_2 \ \mathbf{e}'_3] = [\mathbf{e}_1 \ \mathbf{e}_2 \ \mathbf{e}_3]X \quad (1)$$

OR

$$\mathbf{e}' = \mathbf{e}X. \quad (2)$$

In these equations,  $[\mathbf{e}_1 \ \mathbf{e}_2 \ \mathbf{e}_3] \equiv \mathbf{e}$  is to be regarded as a row matrix. When the orientation matrix  $X$  is known, one can determine the angles between any directions or planes in the two lattices and find a correlation between the lattices in terms of the product of a pure rotation and a pure deformation (e.g. Christian, 1975). One can also study the possibility of coincident points between the two lattices and whether such points define a three-, two- or one-dimensional lattice and determine the degree of coincidence in each case. Methods of solving these problems have been developed by Grimmer (1976) and Fortes (1983b). Finally, it is possible to determine the 0-lattice from the matrix  $X$  (Bollman, 1970) and calculate the misfit dislocation content of an interface between the two crystals (Bollmann, 1970; Knowles, 1982).